# Swelling of $K^+$, $Na^+$ and $Ca^{2+}$-montmorillonites and hydration of interlayer cations: a molecular dynamics simulation*

Liu Tao(刘 涛)[a], Tian Xiao-Feng(田晓峰)[a], Zhao Yu(赵 宇)[b], and Gao Tao(高 涛)[a]†

[a] *Institute of Atomic and Molecular Physics, Sichuan University, Chengdu* 610065, *China*

[b] *Institute of Mountain Hazards & Environment, Chinese Academy of Sciences & Ministry of Water Conservancy, Chengdu* 610041, *China*

(Received 6 November 2009; revised manuscript received 8 April 2010)

This paper performs molecular dynamics simulations to investigate the role of the monovalent cations K, Na and the divalent cation Ca on the stability and swelling of montmorillonite. The recently developed CLAYFF force field is used to predict the basal spacing as a function of the water content in the interlayer. The simulations reproduced the swelling pattern of these montmorillonites, suggesting a mechanism of their hydration different ($K^+ < Na^+ < Ca^{2+}$) from that of $K^+$-, $Na^+$-, and $Ca^{2+}$-montmorillonites. In particular, these results indicate that the valence of the cations has the larger impact on the behaviour of clay–water systems. It also finds that the differences in size and hydration energy of $K^+$, $Na^+$ and $Ca^{2+}$ ions have strong implications for the structure of interlayer. This leads to the differences in the layer spacings of the simulated $K^+$-, $Na^+$-, and $Ca^{2+}$-montmorillonites. Furthermore, these simulations show that the K cations interact strongly with the clay sheets for the dehydrated clay sheets, but for the hydrated clays the Ca cations interact clearly strongly with the clay sheets.

**Keywords:** montmorillonite, molecular dynamics simulation, swelling, hydration energy

**PACC:** 9160, 9160W, 8715D, 7115Q

## 1. Introduction

Montmorillonite is among the most common clay minerals and has received much attention recently owing to its physical and chemical properties.[1−6] Montmorillonite is important in a number of technological and industrial applications such as catalytic activity, adsorbents in environmental engineering, and waste disposal.[7−10] Among clay minerals, montmorillonite is a 2:1 clay mineral, consisting of two tetrahedral sheets separated by one octahedral sheet. Tetrahedral substitution of Si by Al in two tetrahedral sheets and/or octahedral substitutions of Al by Mg in a central octahedral sheet make the clay platelets negatively charged, which are compensated by interlayer ions. At the same time, the capacity of montmorillonite to incorporate water into its interlayer regions and cause clay swelling are of central interest.

Although the stability and swelling properties of clays saturated with sodium cation were studied in previous simulation works,[11−16] no simulation study has given consideration to the question of how the monovalent and divalent cations are affecting the swelling pattern of $K^+$-, $Na^+$-, and $Ca^{2+}$-montmorillonites. Generally, clay minerals lack long range order due to their small platelet size and stacking behaviour, and therefore they are difficult to characterize accurately by experimental methods. Molecular simulation is an ideal way of gaining insight at an atomistic level into the molecular structure and dynamics of clay minerals,[17−21] in particular, the current interest in the swelling of montmorillonite clays and hydration of interlayer cations.

In the past decade, molecular dynamics (MD) simulations were widely employed to study the clay-fluid systems.[22−26] In this paper, we carried out comprehensive MD simulations on $K^+$-, $Na^+$-, and $Ca^{2+}$-montmorillonites with a wide range of water contents in order to obtain the structural and dynamic properties of these montmorillonites. At the same time, we are able to obtain detailed insight into the variation of the interlayer spacing and molecular structure with changing water content by increasing the water content in small step. In the present work, Wyoming montmorillonites were selected as model montmoril-

*Project supported by the Key Laboratory of Mountain Hazards and Earth Surface Processes, the Chinese Academy of Sciences.
†Corresponding author. E-mail: gaotao2010@gmail.com
© 2010 Chinese Physical Society and IOP Publishing Ltd

lonite and the advanced CLAYFF force field was employed. Swelling curves, spatial distributions, swelling patterns and mobility of interlayer cations and water were derived.

The structure of the paper is as follows. In the next section, we describe the simulation details. In Section 3 we present the results and discussion, and finally we summarize and conclude our analysis in Section 4.

# 2. Model and method

## 2.1. Force-field and simulation details

All MD simulations were carried out by using the LAMMPS package,[27] and the recently developed CLAYFF force field[28] was used to describe the interatomic interactions. The CLAYFF has been shown to be highly effective in the simulation of hydrated and multicomponent mineral systems and their interfaces with aqueous solutions. The interatomic potential in the CLAYFF force field is derived from parametrization incorporating structural and spectroscopic data for a variety of simply hydrated compounds. In order to permit simulation of complex disordered clay systems, all atoms are represented as point charges and allowed complete translational freedom within this force field framework. Metal–oxygen interactions are based on a simple Lennard–Jone potential combined with electrostatics. The empirical parameters are optimized on the base of known mineral structures, and the partial atomic charges are derived from periodic density functional theory (DFT) quantum chemical calculations of simple oxide, hydroxide, and oxyhydroxide model compound.[28] Oxygen and hydroxyl charges vary with nearest-neighbour cation substitution. The bond stretch and angle bend terms with flexibility of the OH are represented in the clay lattice as harmonic terms. For the water behaviour, the flexible version of the SPC (single point charge) model is used.[29] Compared to the more complex water models (e.g., TIP4P, BJH), the SPC model is relatively simple in having partial charges centred directly on each of three atoms, and the short-range interactions represented by a simple Lennard–Jones term. The simulation was run for at 1 ns at 300 K and 1 atm by using an isobaric–isothermal (NPT) ensemble in which the temperature and pressure were maintained via a Nose–Hoover thermobraostat.

## 2.2. Model structures

We simulated a Wyoming montmorillonite with the unitcell formula $X_y$ $(Si_{7.75}Al_{0.25})$ $(Al_{3.5}Mg_{0.5})$ $O_{20}(OH)_4{\cdot}nH_2O$, where $X_y = K_{0.75}$ for K, Na-montmorillonites, and $X_y = Ca_{0.375}$ for Ca-montmorillonite. To model a montmorillonite particle, three-dimensional periodic boundary conditions were applied to a simulation box composed of 16 (4×4×1) unit cells, having horizontal dimensions of $L_x \times L_y$ and representing halves of two montmorillonite layers with an interlayer space in between.

All the simulations were first run for a total of $2\times10^5$ time steps to reach equilibrium configurations before statistical averages were taken. Once equilibrium was achieved, production runs of a total of $10^5$ time steps were run with averages accumulated in blocks of $10^5$ time steps. We chose to output the atomic positions every 2.0 ps during production runs. From this datum, radial distribution functions and atomic density profiles were calculated.

# 3. Results and discussion

## 3.1. Swelling behaviours and interlayer structures

The interlayer spacings of $K^+$-, $Na^+$-, and $Ca^{2+}$-montmorillonites have been calculated as a function of water content increasing from 0 to 224 molecules as shown in Fig. 1. In the simulations, figure 1 indicates that the $K^+$-, $Ca^{2+}$-montmorillonites exhibit an overall smaller interlayer space than the $Na^+$-montmorillonite. Similar results to ours were obtained for the $K^+$-, $Na^+$- and $Ca^{2+}$-montmorillonites system by using Monte Carlo simulations.[30−33] For the dry state (no water molecules in the interlayer), our simulations yield a *d*-spacing $D = 10.07$ Å (1 Å = 0.1 nm) for Na–Wyoming, and $D = 9.68$ Å for Ca–Wyoming. The experimental values have been reported by Boek *et al.*[34] and Rutherford *et al.*[35] for the dry state of two $Na^+$- and $Ca^{2+}$-montmorillonites, the results are similar to ours, which are $D = 10.17$ Å and $D = 9.70$ Å. In the meanwhile, we found that Ca-montmorillonite exhibits smaller basal spacing than K-montmorillonite as a function of the water content.

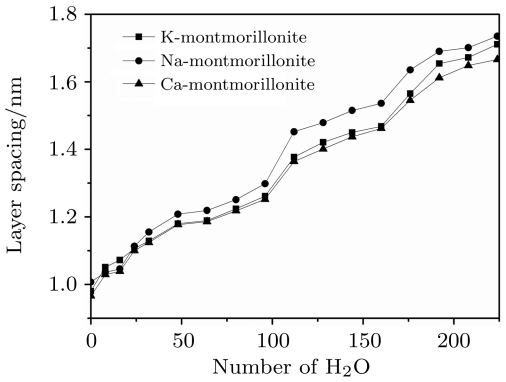



**Fig. 1.** Swelling curves of the potassium-, sodium-, and calcium-montmorillonite clay showing the dependence of the layer spacing on the water molecules of the clay.

Comparing the curves in Fig. 1 we see that the presence of the potassium and calcium ions has a dramatic effect on the interlayer spacing, moreover, K and Ca clays present smaller basal spacings than Na clays in present work. We note that the valence of the cations has the large impact in the behaviour of clay-water systems. These results indicate that Na-montmorillonite has a more open structure than K- and Ca-montmorillonites under similar conditions. The K- and Ca-clays exhibit a tighter structure, thereby yielding more compact and stable clay particles at the macroscopic level.

In determining the swelling curves, three representative water contents corresponding to 64, 128 and 224 water molecules were selected to study the structural and dynamical behaviours of the interlayer species. Figures 2, 3 and 4 show the density profiles of the water oxygens and the cations for their corresponding three values of the water content, namely, $N_{\rm w} = 64$ (a), $N_{\rm w} = 128$ (b), and $N_{\rm w} = 224$ (c), respectively. Note that for $N_{\rm w} = 64$ the water in the interlayer forms a single layer, whereas two layers of water are formed for $N_{\rm w} = 128$, and $N_{\rm w} = 224$ for three layers of water formation. Our simulations for $K^+$-, $Na^+$-, and $Ca^{2+}$-Wyoming montmorillonites indicate that the cations are surrounded by water molecules for most water contents. These results indicate that, as the external applied pressure on the system decreases and external environment of the water contents increases, the stable states of the clay–water systems proceed from the dry state to form one, two, and three layers of water, until the bulk limit is reached. In the present case, we also find that for both K- and Ca-montmorillonites the K and Ca cations are hydrated.

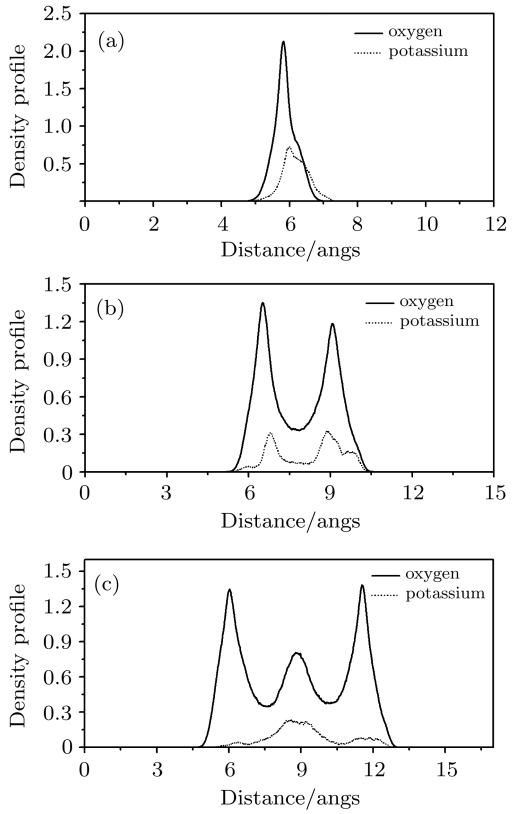



**Fig. 2.** Density profiles for water oxygens and cations (potassium) for water contents 64 (a), 128 (b), and 224 (c), respectively.

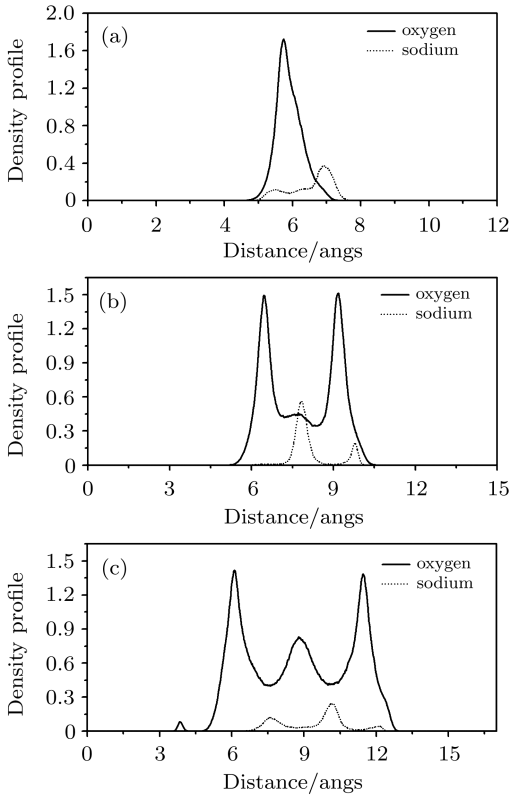



**Fig. 3.** Density profiles for water oxygens and cations (sodium) for water contents 64 (a), 128 (b), and 224 (c), respectively.

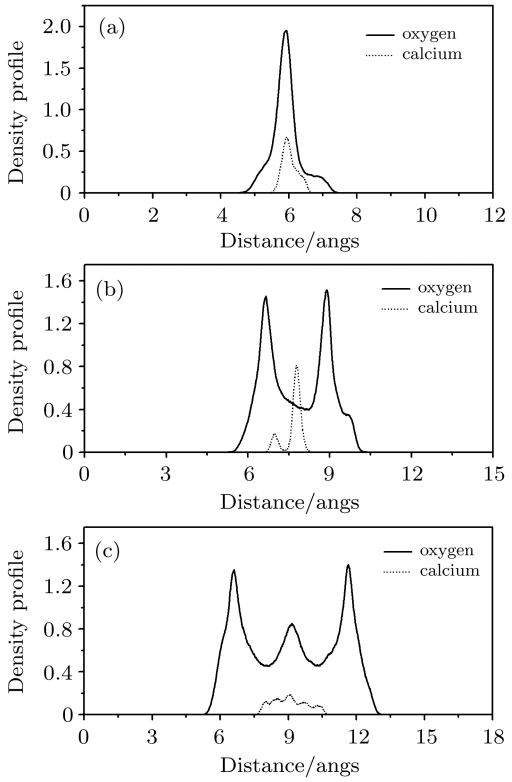



**Fig. 4.** Density profiles for water oxygens and cations (calcium) for water contents 64 (a), 128 (b), and 224 (c), respectively.

In Fig. 2, at low water content (about 64 molecules) only one cation layer is present, splitting up into two parts upon further hydration. These ions are distributed roughly equally in two planes offset from the interlayer midplane. When the water content is increased above 224 molecules, this central layer splits up into three peaks, possibly related to the start of a "diffuse ion swarm". However, for the sodium and calcium ions (Figs. 3 and and 4), the general picture is different from the $K^+$ ions. From 0 to 64 water molecules in the interlayer spacing, the $Ca^{2+}$ ions remain in a single layer in the midplane region (Fig. 4(a)). However, the density peaks of $Na^+$ ions appear on the right-hand side (Fig. 3(a)). Then an asymmetry in the density profiles is shown upon further increase of the water content, for both Na and Ca: although most of the Na and Ca ions distributed in the central part of the interlayer, the smaller density peaks on the right-hand side of Na ions is farther than the ones on the left-hand side of Ca ions (Figs. 3(b) and 4(b)). This may explain the greater distance of the layer-spacing of Na ions. Finally, the Ca cations are mostly distributed in the central part of the interlayer with the increase of the water contents, where they are fully surrounded by water molecules in Fig. 4(c).

The $K^+$-, $Na^+$-, and $Ca^{2+}$-montmorillonites display the same qualitative features when the water density profiles are considered. As we increase water molecules from 0 to 64, the water monolayer in the interlayer spacing builds up, giving rise to one single peak in the density profile. Then when the water content is increased above 128 molecules, a two-layer hydrate originates. Finally, for 224 molecules, the start of a third layer can be observed, more diffusely arranged around the midplane. Possibly it is related to the development of a diffuse ion swarm. Similar results were obtained previously from Delville's simulations.[36]

## 3.2. Interaction between interlayer cations and water

As a prerequisite, such a detailed analysis requires the interlayer cation–water–oxygen radial distribution functions (RDFs), which are presented in Fig. 5. For Na- and Ca-montmorillonites, the first-neighbour peak is centred near 2.48 Å and 2.42 Å in one-, two-, and three-hydrates, respectively. However, for K-montmorillonite, the first-neighbour peak is shifted to 2.75 Å in one-, two, and three-hydrates. These results reflect the shift owing to the presence of interlayer different cations. Moreover, these results show that when hydrated within clays, $Ca^{2+}$ and $Na^+$ behaves as in bulk water. Similar results to ours were obtained for the hydrated Ca- and Na-montmorillonites system by Monte Carlo simulations.[30,37]

Furthermore, comparing with the hydration shell around the $Na^+$ and $Ca^{2+}$ cations, we found that the first-neighbour cation–oxygens are assembled more densely than those in the case of the $K^+$ cation, which is the reason why the first-neighbour peaks of the Na–O and Ca–O RDF are centred near 2.48 Å Na-montmorillonite and 2.42 Å Ca-montmorillonite in comparison with 2.75 Å for K-montmorillonite.

The relatively sharp appearance of this peak in one-, two-, and three-hydrate states of Na- and Ca-montmorillonites, in comparison with that of the corresponding peak for K-montmorillonite, suggesting that the Na and Ca cations have strongly hydration energy than the K cation in the interlayer spacing. Meanwhile, compared to these cations, $K^+$ has lower hydration energy, which explains the greater distance of the first-neighbour peak in the one-, two-, and three-hydrations.

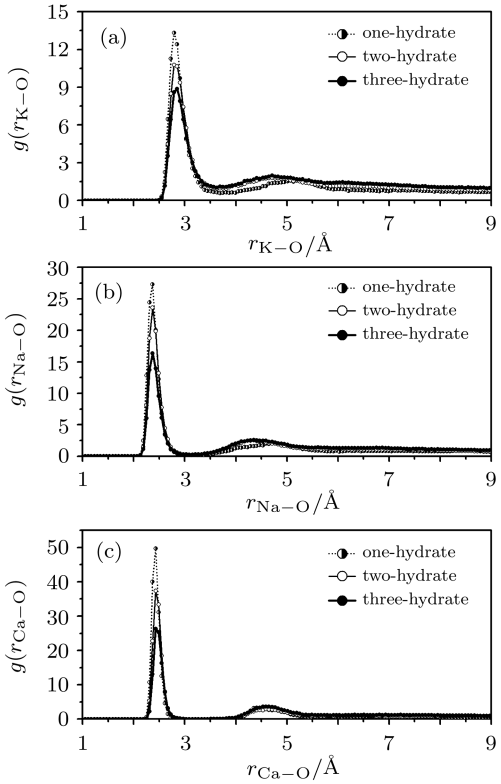



**Fig. 5.** Cations–water oxygen atoms RDF in the one-hydrate, two-hydrate, and three-hydrate states: (a) for K-montmorillonite; (b) for Na-montmorillonite; and (c) Ca-montmorillonite at 64, 128, and 224 water molecules, respectively.

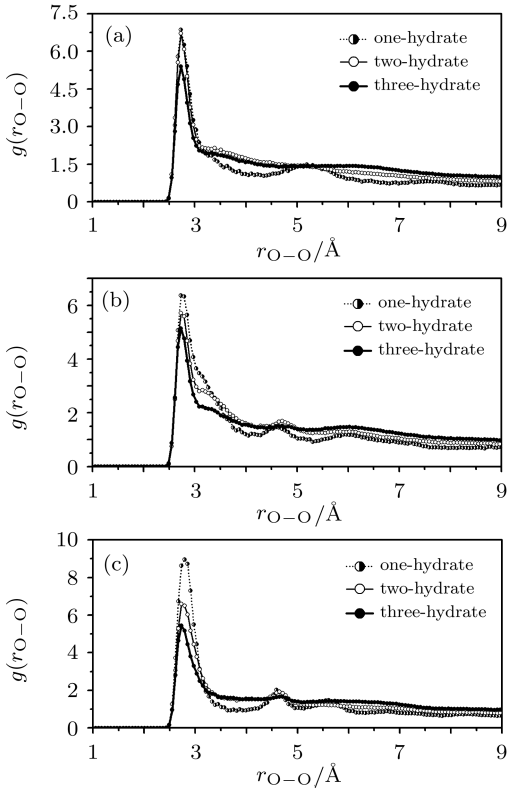



**Fig. 6.** The O–O RDFs in the one-hydrate, two-hydrate, and three-hydrate states at 64, 128, and 224 water molecules, respectively: (a) for Na-montmorillonite; (b) for K-montmorillonite; and (c) for Ca-montmorillonite.

## 3.3. Structure of interlayer water

To allow a more detailed analysis of the effect of interlayer cations on interlayer water, figure 6 compares the water structures of one-, two-, and three-hydrates of $K^+$-, $Na^+$-, and $Ca^{2+}$-montmorillonites, as represented by the water oxygen–water oxygen (O–O) RDFs. The pairs of water oxygens contributing to the first- and second-neighbour peaks in the one-hydrate state are depicted for clarity also in Fig. 6. For K-montmorillonite, the first-neighbour peak is centred near 2.82 Å in one-, two-, and three-hydrates. For Na-montmorillonite, the first-neighbour peak is centred near 2.80 Å in one-, two-, and three-hydrates. However, the first-neighbour peak is shifted to 2.70 Å in two- and three-hydrates for Ca-montmorillonite, but is centred near 2.80 Å in one-hydrate. It is apparent that the shift in two- and three-hydrates occurs because water molecules are in the hydration shells of $Ca^{2+}$ cations, which would compensate for this effect of cation hydration on water structure.

In the more compact hydration shell around the $Na^+$ (or $Ca^{2+}$) cation, the second-neighbour water oxygen atoms are assembled more densely than in the case of the $K^+$ cation, which is the reason why the second-neighbour peak of the O–O RDF is centred near 4.6 Å for Na-montmorillonite in comparison with 5.2 Å for K-montmorillonite. The relatively sharp appearance of this peak in the one-hydrate state of K-, Na-, and Ca-montmorillonites and the two-hydrate state of Na- and Ca-montmorillonites, is apparently another effect of cation hydration, as suggested in Ref. [18]. As interlayer water content increases, in the three-hydrate state of K-, Na-, and Ca-montmorillonites, this peak broadens and becomes similar to that in bulk liquid.

## 3.4. Interaction between interlayer cations and clay oxygen atoms

It is well known that the interaction of the clay cations with their environment depends on non-bonding electrostatic and van der Waals potentials. As shown in Fig. 7, the RDFs between the cations and the clay tetrahedral oxygen atoms of the dehy-

drated clays clearly show structure. By contrast, we can see that this structure tends to disappear for the hydrated clays. This can be explained as follows. The cations interact strongly with the clay sheets in dehydrated clays. However, in the case of hydrated clays, the cations are solvated by water and are more likely to diffuse within the clay galleries. In the dehydrated clays, the first-neighbour peak of K-montmorillonite is relatively sharp in comparison with that of the corresponding peaks for Na- and Ca-montmorillonites. However, in the case of hydrated clays, the first-neighbour peak of Ca-montmorillonite is stronger in comparison with that of the first-neighbour peaks for K- and Na-montmorillonites ($Na^+ < K^+ < Ca^{2+}$).

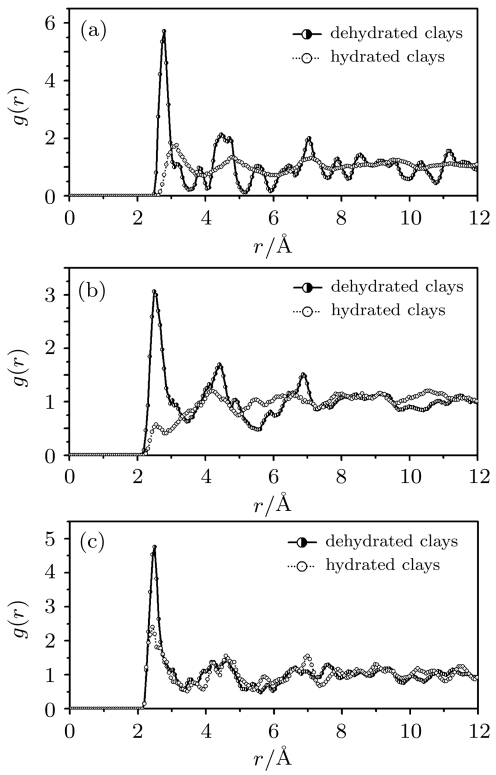



**Fig. 7.** Cations–clay oxygen atoms RDF in the dehydrated clays and hydrated clays states: (a) for K-montmorillonite; (b) for Na-montmorillonite; and (c) for Ca-montmorillonite, respectively.

Furthermore, compared to the small alkali cations, $Ca^{2+}$ has higher hrdration energy but $K^+$ has lower hydration energy, which explains the less distance of the first hydration sphere for $Ca^{2+}$ ions and the greater distance of the first hydration sphere for $K^+$ ions (Fig. 7). Thereby, the interlayer space of the Ca-montmorillonite is smaller than that of the K-montmorillonite.

# 4. Conclusions

In this work we have presented an MD computer simulation of $K^+$-, $Na^+$-, and $Ca^{2+}$-saturated montmorillonites using the recently developed CLAYFF force field. First, we presented the swelling of $K^+$-, $Na^+$-, and $Ca^{2+}$-montmorillonites and compared it with previous experimental and theoretic results. We found that Ca-montmorillonite exhibits less swelling than Na- and K-montmorillonites for a given water content. Second, we compared K-saturated clays and Na-, Ca-saturated clays and found that the K, Ca cations have a large influence on the swelling, inhibiting it with respect to that predicted for the Na cation. These simulations clearly show that the cations are solvated by water in present work. In future developments, we plan to compute the elastic properties and the diffusion coefficients of the water molecules and cations for these systems.

The results of the present study show that the higher the hydration energy of the interlayer cation, the greater is this difference. Meanwhile, the hydration energy of the Ca cation is stronger than that of the Na cation, especially the K cation. Furthermore, for the dehydrated clays, comparing with the RDFs between the cations and the clay oxygen atoms (Fig. 7), we show that the K cations interact strongly with the clay sheets. However, for the hydrated clays, figure 7 shows that the Ca cations interact clearly strongly with the clay sheets.

# References

[1] Velde B 1995 *Origin and Mineralogy of Clays* (New York: Springer)
[2] Perkins D 1998 *Mineralogy* (New Jersey: Prentice Hall)
[3] Giannelis E P 1996 *Adv. Mater.* **8** 29
[4] Alexandre M and Dubois P 2000 *Mater. Sci. Eng.* **28** 1
[5] Lebaron P C, Wang Z and Pinnavaia T 1999 *J. Appl. Clay Sci.* **15** 11
[6] Greenwell H C, Jones W, Voveney P V and Stackhouse S 2006 *J. Mater. Chem.* **16** 708
[7] Teng B K G 1974 *The Chemistry of Clay–Organic Reactions* (New York: Wiley)
[8] Grim R E 1962 *Applied Clay Mineralogy* (New York: McGraw-Hill)
[9] Bleam W F 1993 *Rev. Geophys.* **31** 51
[10] Gong B A and Qi S M 1995 *Acta Phys. Sin.* **44** 157 (in Chinese)

[11] Skipper N T, Chou Chang F and Sposito G 1995 *Clays Clay Miner.* **43** 285

[12] Karaborni S, Smit B, Heidug W, Urai J and Oort E van *Science* 1996 **271** 1102

[13] Chávez-Páez M, Workum K Van, DePablo L and DEPablo J J 2001 *J. Chem. Phys.* **114** 1405

[14] Greathous J A and Storm E W 2002 *Mol. Simul.* **28** 633

[15] Greathouse J A, Refson K and Sposito G 2000 *J. Am. Chem. Phys.* **94** 7434

[16] Fang Q H, Huang S P, Liu Z P and Wang W C 2004 *Acta Chinm. Sin.* **62** 2407 (in Chinese)

[17] Skipper N T, Chang F R C and Sposito G 1995 *Clays. Clay. Miner.* **43** 285

[18] Skipper N T, Chang F R C and Sposito G 1995 *Clays. Clay. Miner.* **43** 294

[19] Stackhous S, Coveney P V and Sandre E 2001 *J. Am. Chem. Soc.* **123** 11764

[20] He M C, Fang Z J and Zhang P 2009 *Chin. Phys.* B **18** 2933

[21] He H P, Galy J and Gerard J F 2005 *J. Phys. Chem.* B **109** 13301

[22] Shao J L, Qin C S and Wang P 2009 *Acta Phys. Sin.* **58** 1936 (in Chinese)

[23] Skipper N T, Lock P A, Titiloyer J O, Mirza Z A, Howells W S and Fernandez-Alonso F 2006 *Chem. Geol.* **230** 182

[24] Li X, Hu Y Z and Jiang L 2008 *Chin. Phys.* B **17** 3035

[25] Xie H X, Wang C Y, Yu T and Du J P 2009 *Chin. Phys.* B **18** 251

[26] Li M L, Zhang D S, Fu H N, Yao X Y, Li X W, Duan C, Yan Y P, Mu Y, Chen H and Sun M H 2008 *Acta Phys. Sin.* **57** 7157 (in Chinese)

[27] Plimpton S J 1995 *J. Comput. Phys.* **117** 1

[28] Cygan R T, Liang J J and Kalinichev A G 2004 *J. Phys. Chem.* B **108** 1255

[29] Berendsen H J C, Postma J P M, van Gunsteren W F and Hermans J 1981 *Interaction Models for Water in Relation to Protein Hydration,* in *Intermolecular Forces*, ed. Pullman B (Amsterdam: D Reidel) p. 331

[30] Chávez-Páez M and Workum K V 2001 *J. Chem. Phys.* **114** 1405

[31] Pablo L De, Chávez M L, Sum A K and De Pablo J J 2004 *J. Chem. Phys.* **120** 939

[32] Boek E S, Coveney P V and Skipper N T 1995 *J. Am. Chem. Soc.* **117** 12608

[33] Chávez-Páez M, Pablo L De and De Pablo J J 2004 *J. Chem. Phys.* **114** 24

[34] Boek E S, Conevey P V and Skipper N T 1995 *Langmuir* **11** 4629

[35] Rutherford D W, Chiou C T and Eberl D D 1997 *Clays Clay Miner.* **45** 534

[36] Delville A 1992 *Langmuir* **8** 1796

[37] Marry V, Turc P, Cartailler T and Levesque D 2002 *J. Chem. Phys.* **117** 3454